Paper No.
C2025-00474

AMPP ANNUAL CONFERENCE + EXPO
APRIL 6-10, 2025 | NASHVILLE, TENNESSEE

Validation of Modern CFD Software in Backward Facing Step and Glass Cell Geometries

Adam Cutright, Bruce Brown, David Young

Institute for Corrosion & Multiphase Technology (ICMT)

Department of Chemical and Biomolecular Engineering, Ohio University

Athens, OH 45701

United States

ABSTRACT

The key issues with the utilization of CFD software for corrosion prediction in complex geometries are the method of implementation and confidence in the results obtained. To overcome these issues, simulations have been performed which replicate systems from which experimental data has also been obtained which allows for the direct comparison of the experimental data with predictions obtained from the simulations. The appropriate turbulence models are selected to account for the hydrodynamics of the system, mass transfer models with chemical and electrochemical reactions are input into the software which allows for the simulation of both water chemistry and corrosion.

Presented herein is work investigating corrosion phenomena in a backward facing step, similar to a sudden pipe expansion, as well as a 2L glass cell, a common geometry for laboratory testing. In both geometries hydrodynamics, mass transfer, and electrochemistry have been simulated at a variety of conditions; the accuracy of the results were confirmed through comparison with experimental data. Both geometries showed a high degree of agreement between the simulations and the experimental work, indicating that the methodology is viable to be used in other geometries.

Key words: Corrosion mechanisms, Corrosion rate, Oil and gas, Carbon dioxide, CFD

INTRODUCTION

In the oil and gas industry, use of models for prediction of corrosion to develop appropriate mitigation strategies is widespread. These models often rely on dimensionless number mass transfer correlations in order to predict pipe flow conditions which are used to make the corrosion

predictions. These correlations are effective in laminar and turbulent, single phase, straight pipe flow. The downside to this approach is that in systems where these correlations do not currently exist, such as for many multiphase flow systems or when a more complex geometry is present (bends, valves, fittings, obstacles), these models cannot accurately predict corrosion.

To model corrosion in such systems, CFD (computational fluid dynamics) software can be implemented along with the appropriate understanding of the corrosion mechanisms. CFD software functions by taking a 2D or 3D geometry and breaking it down into a system of points at which flow variables and other system variables like temperature, pressure, species concentration will be calculated; this process is also known as discretization or meshing. Once the mesh has been created for the system, the software then solves a number of equations simultaneously at each point inside the system using numerical methods. The equations solved will partly depend on what system variables are of interest to the user, those that must always be solved are the continuity equation, and the Navier-Stokes equation which are shown below. The Navier-Stokes equation is a set of 3 equations which describes the momentum transfer in a fluid system.

$$\frac{\partial \rho}{\partial t} + \frac{\partial (\rho u_i)}{\partial x_i} = 0 \tag{1}$$

$$\frac{\partial \rho u_j}{\partial t} + \frac{\partial}{\partial x_i}(\rho u_j u_i) = \rho f_j - \frac{\partial P}{\partial x_j} + \frac{\partial}{\partial x_i}\left(\mu \frac{\partial u_j}{\partial x_i}\right) + \frac{1}{3}\frac{\partial}{\partial x_j}\left(\mu \frac{\partial u_i}{\partial x_i}\right) \tag{2}$$

In the case of a corrosion calculation the only thing left out in the above equations are the concentrations of species which are relevant to the corrosion reactions. These can be solved for by including the species conservation equation which is shown below.

$$\frac{\partial}{\partial t}(m^s) + \frac{\partial}{\partial x_i}(m^s u_i) = \frac{\partial}{\partial x_i}\left(D^s \frac{\partial m^s}{\partial x_i}\right) + R^s \tag{3}$$

From this point the local concentration of species at any point inside the system can be calculated and utilized in the calculation of the corrosion rate. To calculate the corrosion rate itself, another equation must be solved, this time at the wall where the corrosion occurs. For this, the Butler-Volmer equation, which can be seen below, is implemented. The Butler-Volmer equation is an equation that relates the current related to corrosion with the anodic and cathodic Tafel slopes as well as the potential in the system and concentration of relevant species. This equation is implemented as a boundary condition, boundary conditions play a big role in CFD simulations as these are the ways in which information is transferred into the system, such as specifying a particular velocity or flow rate at an inlet, or a pressure at an outlet.

$$i_F = i_0 \left(\frac{c}{c_{ref}}\right)^n \left[\exp\left(\frac{2.303\eta}{\beta_a}\right) - \exp\left(\frac{2.303\eta}{\beta_c}\right)\right] \tag{4}$$

This implementation allows for the calculation by the CFD software of the current density of the electrochemical corrosion reaction, which can then be transformed into a corrosion rate.

EXPERIMENTAL PROCEDURE

Equipment

- Ansys Fluent™ software

Procedure

For the purposes of this project, the current focus is the verification of hydrodynamics, mass transfer, and electrochemical and chemical reactions in different experimental systems. In order to verify these parameters in these experimental systems, first literature sources are found which provide experimental data in these systems. When direct comparison with experimental data is to be performed, the experimental systems are designed in the CFD software, carefully replicating the significant physical dimensions of the experimental systems used in the literature source. The parameters of the simulation are input to exactly recreate the conditions seen in the experiments being referenced. The relevant simulation results are then compared with the data present in the literature to determine the accuracy of the simulated results.

RESULTS DISCUSSION

Sudden Pipe Expansion

The first experimental system simulated is the sudden pipe expansion, where a pipe undergoes an immediate increase in diameter. To verify the hydrodynamics of the simulations data was taken from Khezzar.[1] The experiments in this work to be compared against were axisymmetric and so a 2D axisymmetric simulation was used. The geometry and mesh along with relevant physical measurements can be seen below in Figure 1 and Figure 2.

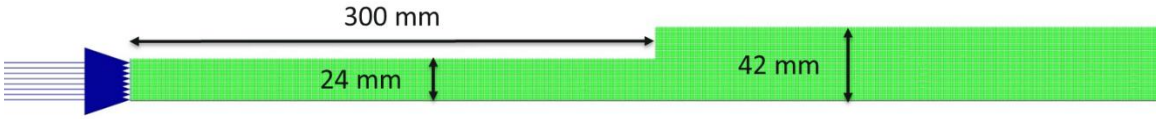

Figure 1. 2D mesh for sudden pipe expansion simulation.

Figure 2. Magnified view of sudden pipe expansion mesh.

To start modeling, only hydrodynamics were considered, where data from Khezzar showing the reattachment length (after the expansion) as a function of the upstream Reynolds number (prior to the expansion) was used.[1] After the expansion it is expected that the flow will separate causing a recirculation zone, the bulk of the flow towards the center of the pipe will continue moving forward, while the flow near the edges will flow backwards; the reattachment length is the distance after which all of the flow moves forward, with the flow towards the edges that was moving backwards reattaching itself to the bulk flow.

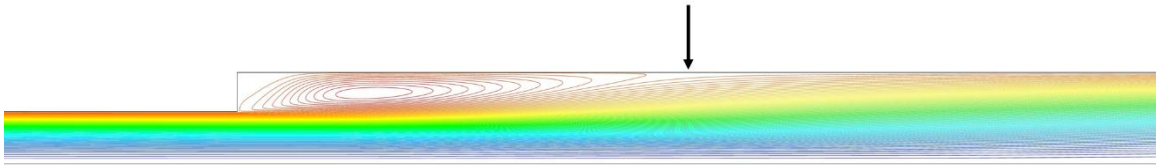

Figure 3. Contour of stream function indicating the general flow pattern with the location of reattachment indicated by arrow.

By using the geometry shown in Figure 1, and adjusting the inlet velocity to achieve the desired value of Reynolds number, the simulations were performed at all Reynolds numbers tested in the experimental system. Given that the Reynolds values simulated span laminar, transitional, and turbulent flow, different viscous models were needed for each region. In the laminar flow region, the laminar viscous model was used, in the transitional region the k-ω SST model with low Reynolds number corrections was used, and in the fully turbulent region the k-ω SST model was used. The comparison of the simulated reattachment length, which has been non-dimensionalized with the downstream pipe diameter, for the various Reynolds numbers can be seen below in Figure 4. The agreement between the model and the simulation is very good in both the laminar (first) and turbulent (last) regions, but in the transitional region there is some discrepancy; however, the general trend seen in the experimental data is well replicated by the simulations. The slight discrepancy in the transitional region could indicate that further tuning of the models for this region could be necessary in order to achieve more accurate results.

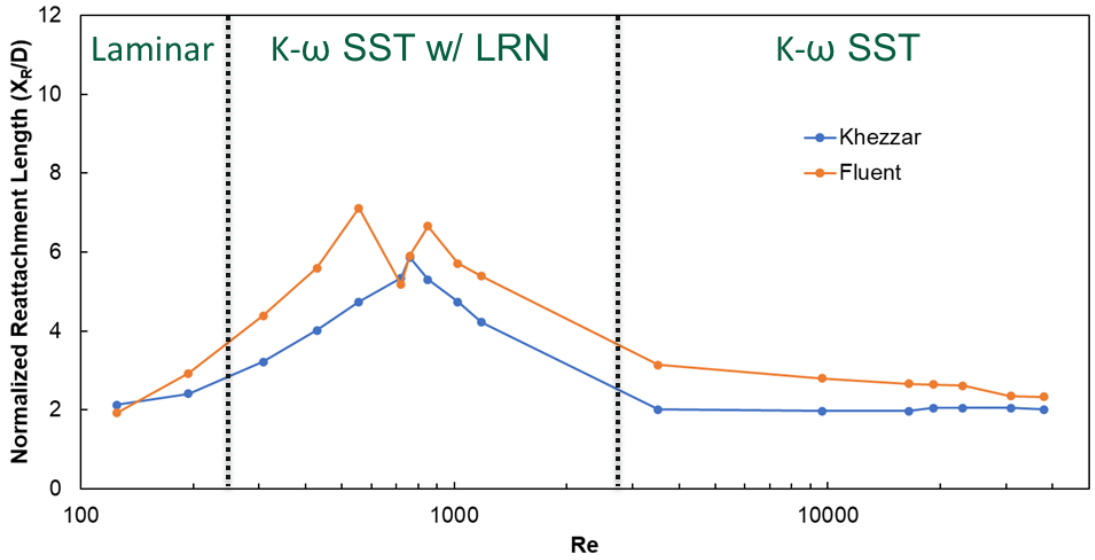

Figure 4. Comparison of simulated and experimental reattachment length at various values of Re.[1]

Additionally, LDA (laser doppler anemometer) data, which is a non-intrusive technique which gives information about the flow velocity and direction of the system, taken from Khezzar[1] which was only reported at the highest value of Reynolds number, can be compared with the simulated data at two locations corresponding to certain distances after the expansion has occurred. Shown below in Figure 5 and Figure 6 are such comparisons. In these figures there is a comparison of the axial velocity which is normalized by the centerline velocity upstream of the expansion on the x-axis, and the radial distance which is normalized by the downstream pipe diameter on the y-axis at different values of x/D, which is a normalized distance in the axial direction of the pipe after the expansion.

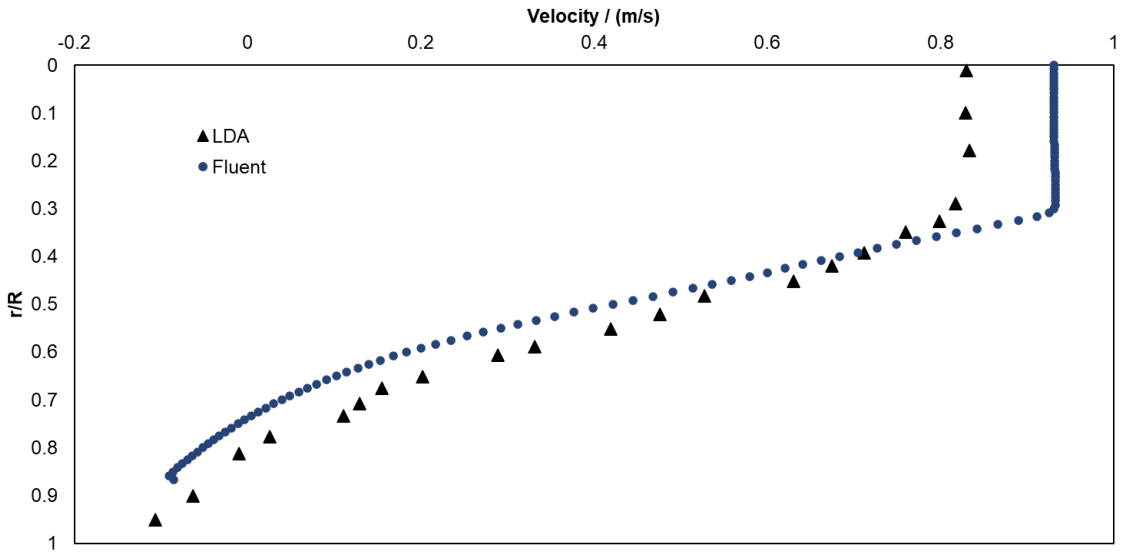

Figure 5. Comparison of LDA data for axial velocity and simulated axial velocity for x/D = 1.5 at Re = 37847.

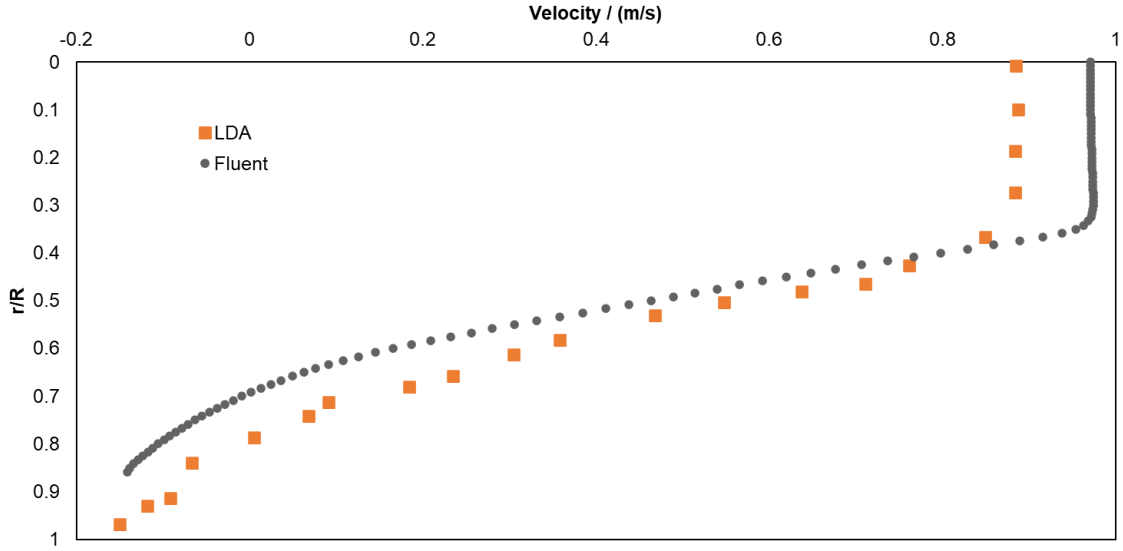

Figure 6. Comparison of LDA data for axial velocity and simulated axial velocity for x/D = 1 at Re = 37847.

It can be seen that in both examples there is a fairly good agreement between the simulations and the LDA data. The trends in the data as r/R approaches 1, which corresponds to the walls of the pipe, are quite similar, and both have achieved a stable velocity at roughly the same r/R value. The slight discrepancy observed at both r/R of 0 and 1 are likely indicative that further tuning of the model is necessary to provide a better agreement with the experimental data.

With the good agreement established in the prediction of the reattachment length, the distance after the expansion at which the flow no longer shows recirculation, and the good ability to predict velocity profiles at various distances confirmed with the LDA measurements, it can be assumed that the CFD software is capable of predicting the hydrodynamics in the given flow geometry.

2-Liter Glass Cell

Simulations were also performed for the 2-liter glass cell geometry which can be seen below in Figure 7, with the corresponding mesh shown in Figure 8. This geometry is commonly used in laboratory experiments, it consists of 5 sample holders evenly spaced around a central impeller which is intended to provide a uniform flow pattern across all 5 samples.

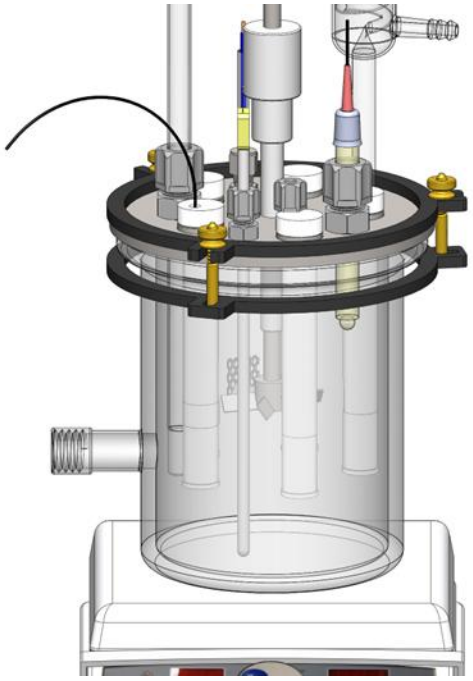

Figure 7. 2 Liter glass cell drawing.

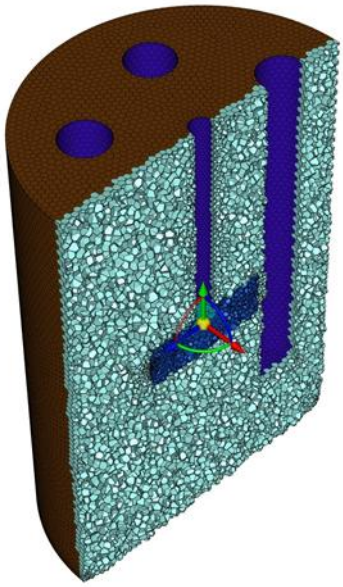

Figure 8. 2-Liter glass cell polyhedral mesh.

It can also be seen in Figure 8 that there are two different regions in the geometry, one region closely surrounding the impeller, and the other consisting of the samples and the bulk fluid. The impeller motion was simulated in the system using the multiple reference frame (MRF) approach where the entire center region of cells containing the impeller is rotated without having to remesh the system as the impeller moves. This region of cells can be assigned a specific rotational speed allowing for simulations of various impeller speeds. The velocity profile in the ZX plane that contains the impeller moving at 75 rpm can be seen below in Figure 9.

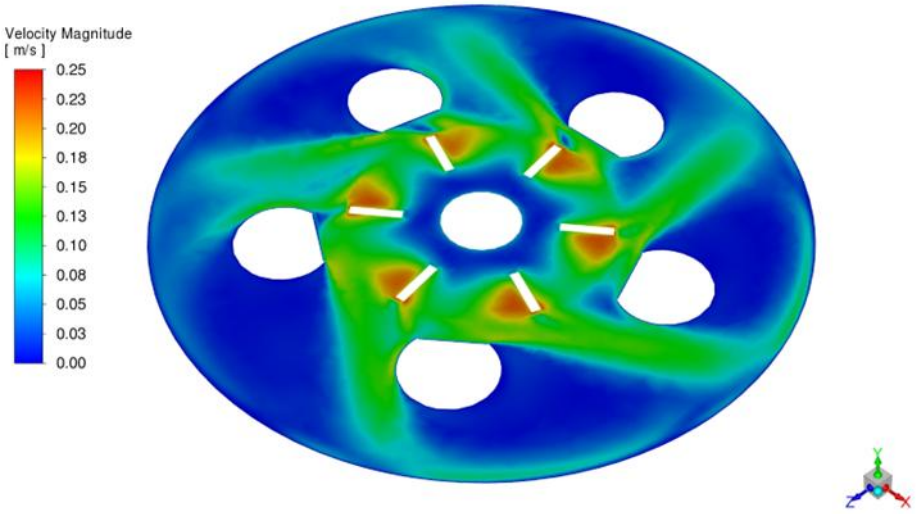

Figure 9. Velocity contour, 75 rpm.

This image shows how the flow is spreading from the impeller and impacting the 5 sample holders spaced evenly around it. Additionally, the flow appears to be very even across each sample, the velocity magnitude in contact with each sample holder appears to be around 0.13 m/s for each sample. It's also important that each sample have a uniform flow across the entirety of the sample, aiming to avoid any uneven corrosion across the samples themselves. In Figure 10 below the wall shear stress on one of the samples can be seen. While there are some areas around the edges which show lower wall shear stress values, the vast majority of the sample has a uniform wall shear stress.

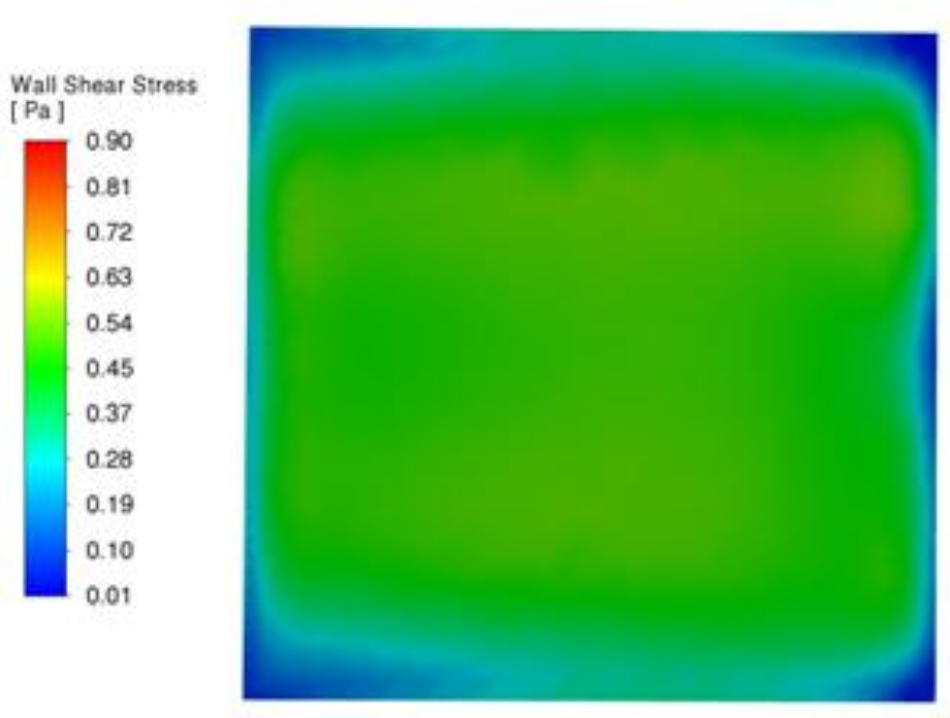

Figure 10. Wall shear stress on sample surface, 75 rpm.

With the hydrodynamics in the system well studied, the next step was to simulate CO_2 corrosion in the system. The parameters for the electrochemical and chemical reactions are specified as shown in Table 1 and

Table **2**. The results were compared with experimental data taken from the same experimental system. A comparison of the experimental data and the simulated corrosion rates can be seen below in Figure 11.

Table 1. Electrochemical parameters for corrosion reactions.[2]

	Hydrogen ion reduction	Iron oxidation
i_0 : exchange current density (A/m^2)	0.03	1
C: species concentration (M)	1E-07	1
Reference mass fraction H+	1E-07	0.001
n: reaction order	0.5	0
β_a : anodic Tafel slope (V)	0.12	0.04
β_c : anodic Tafel slope (V)	0.12	0.04
Equilibrium Potential (V)	-0.24	-0.488

Table 2. Chemical reaction constants for volumetric reactions.[2]

Equation	Forward rate constant	Backward rate constant
CO_2 hydration	0.0348 s^{-1}	24.5 s^{-1}
H_2CO_3 Dissociation	1.9 x 10^7 s^{-1}	4.7 x 10^{10} $M^{-1}s^{-1}$
HCO_3^- Dissociation	181 s^{-1}	3.67 x 10^{12} $M^{-1}s^{-1}$
H_2O Dissociation	0.00126 Ms^{-1}	1.4 x 10^{11} $M^{-1}s^{-1}$

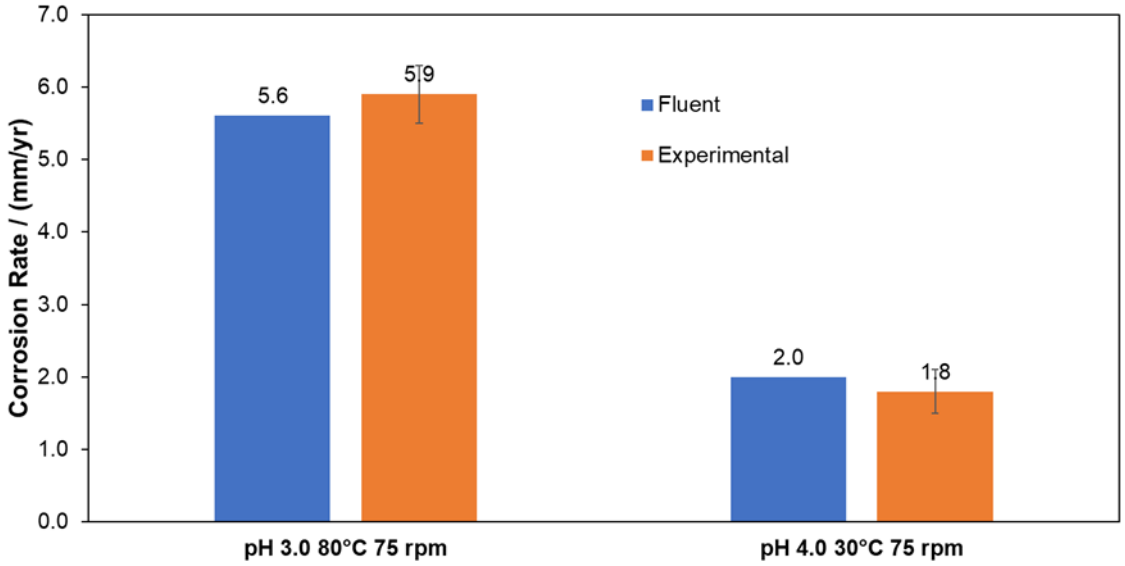

Figure 11. Average corrosion rate at various pH and temperature vs. experimental results from the 2-liter glass cell with impeller.

Figure 11 shows the simulated and experimental values of the corrosion rate are very close for both of the conditions shown, indicating a good ability to accurately simulate and predict the corrosion rates in this specified geometry.

CONCLUSIONS

Flow and CO_2 corrosion were successfully simulated in both the sudden pipe expansion and a 2-liter glass cell. The flow was verified with experimental data in the sudden pipe expansion. The corrosion measurements in the 2-liter glass cell were verified using experimental data.

REFERENCES

(1) Khezzar, L.; Whitelaw, J. H.; Yianneskis, M. Round Sudden-Expansion Flows. *Proc. Inst. Mech. Eng. Part C J. Mech. Eng. Sci.* **1986**, *200* (6), 447–455. https://doi.org/10.1243/PIME_PROC_1986_200_154_02.

(2) ICMT. *Freecorp 2.0 Theoretical Background*; 2018.